



OPEN

Compositional cyber-physical epidemiology of COVID-19

Jin Woo Ro¹, Nathan Allen¹, Weiwei Ai¹, Debi Prasad² & Partha S. Roop¹✉

The COVID-19 pandemic has posed significant challenges globally. Countries have adopted different strategies with varying degrees of success. Epidemiologists are studying the impact of government actions using scenario analysis. However, the interactions between the government policy and the disease dynamics are not formally captured. We, for the first time, formally study the interaction between the disease dynamics, which is modelled as a physical process, and the government policy, which is modelled as the adjoining controller. Our approach enables compositionality, where either the plant or the controller could be replaced by an alternative model. Our work is inspired by the engineering approach for the design of Cyber-Physical Systems. Consequently, we term the new framework Compositional Cyber-Physical Epidemiology. We created different classes of controllers and applied these to control the disease in New Zealand and Italy. Our controllers closely follow government decisions based on their published data. We not only reproduce the pandemic progression faithfully in New Zealand and Italy but also show the tradeoffs produced by differing control actions.

The ongoing Coronavirus Disease 2019 (COVID-19) presents an unprecedented global crisis with 30,675,675 infections and 954,417 deaths as of 20th September 2020¹. There are now widespread calls for new techniques for intervention, including methods of rapid testing even at the home². While Epidemiologists are studying the dynamics of the diseases using computational models, governments are trying to “flatten the curve”³ to reduce the health impacts. This is achieved through Nonpharmaceutical Interventions (NPIs), such as lockdowns and social distancing methods⁴.

The Majority of the research focus in epidemiology has been on mathematical modelling of the disease dynamics. Many governments, like the New Zealand government, have also worked closely with the scientific community⁵ to arrive at critical decisions. But how can we ascertain which model is better, and in which settings⁶? There exists no clear methodology to formally *capture and classify criteria-based actions of the government*⁷ as mathematical models. Also, *given the wide variability of government actions globally, how can we formally assess them while studying their impact?* This paper tries to provide answers to these questions for the first time, by focusing on the compositional modelling of government actions alongside an epidemiological model of the disease.

While at the policy level there has been minimal engineering thinking to provide solutions, it is evident that the pandemic and its control bear many similarities with the well known engineering domain of Cyber-Physical Systems (CPSs)^{8,9}. In a CPS, a physical process such as the electrical conduction of the human heart (known as the *Plant*) is controlled by an adjoining device such as a pacemaker, also known as a *Controller*¹⁰. This closed-loop system mimics the behaviour of a piece-wise continuous phenomena, where the plant's dynamics is modelled using a set of Ordinary Differential Equations (ODEs). The plant makes discrete mode switches based on the actions of a discrete controller.

In the setting of COVID-19, we may view the plant as the dynamics of disease progression, already modelled faithfully using several epidemiological models^{11,12}. The adjoining controller is a state machine that can induce mode switches in the plant. Such a closed-loop system may be depicted as shown in Fig. 1a and we term this approach Compositional Cyber-Physical Epidemiology (CCPE). Here, the plant provides the state of the pandemic encapsulated as a vector of variables $X(t)$, while the controller affects the state of the plant by trying to alter the value of the reproduction number R_0 , which represents the average number of new infections for each infectious person.

There is recent evidence that such engineering thinking may have relevance for COVID-19. The Institute of Electrical and Electronics Engineers (IEEE) published an article citing the benefits of the application of such feedback control theory¹³, which is evidence of concurrent thinking along our lines. However, their work is primarily based on studying the impact of fictitious controllers over a simple disease model, without considering the actual data from the current pandemic.

¹Department of Electrical, Computer and Software Engineering, University of Auckland, Auckland, New Zealand. ²Faculty of Medical and Health Sciences, University of Auckland, Auckland, New Zealand. ✉email: p.roop@auckland.ac.nz

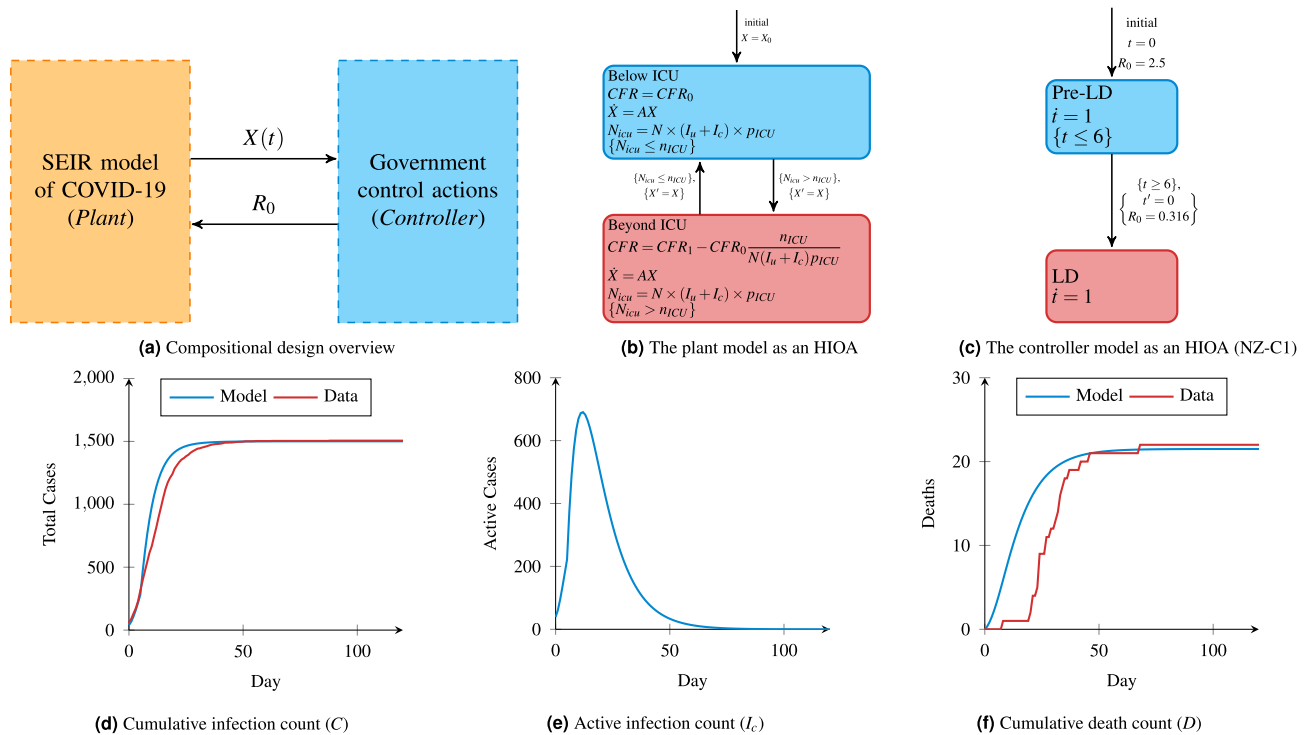


Figure 1. The proposed compositional design of Compositional Cyber-Physical Epidemiology and simulation results. For (d–f), day 0 corresponds to 20th March 2020. For (d,f) these numbers are compared with the available New Zealand data.

This paper advocates that a compositional design approach is needed to include the NPI techniques with the existing epidemiological models. Such an approach, which we term *CCPE*, would allow for the creation of more realistic models which can answer more questions than any existing individual model⁶. This can be used in the decision making of a government, with the goal of both minimising the death toll while reducing the economic impact of any restrictions.

We use Susceptible, Exposed, Infected, Removed (SEIR) model^{11,12} for the illustration of our methodology, while stressing that the developed methodology is amenable to any other dynamical model based on ODEs. The SEIR model incorporates coupled ODEs, and has been utilised previously in the context of COVID-19¹⁴. These ODEs capture the progression of a disease through the population, as people become infected, progress through their infection, and infect others. SEIR models include variables which represent the population during an epidemic which can be in a range of states: susceptible (*S*), exposed (*E*), pre-symptomatic (*P*), infectious (*I*), recovered (*R*) and deaths (*D*). The infected and recovered cases are further categorized into untested (*I_u*, *R_u*) and confirmed cases (*I_c*, *R_c*) to enable control mechanisms which are specific to confirmed cases. The key parameter determining if a virus can cause an epidemic is the reproduction number R_0 and depends on both the transmissibility of the virus and social distancing. For $R_0 > 1$ the virus will spread until herd immunity has been established, while for $R_0 < 1$ the transmission will progressively decay until the virus is eradicated¹². In addition to R_0 , further parameters are used for capturing aspects such as the fatality rate and testing rate.

Government interventions can be used to modify each of these parameters such as the use of NPIs to reduce the reproduction number, or increased testing to isolate more confirmed cases. These responses vary between countries and typically vary over time depending on the local situation^{2,15}. For example, New Zealand acted with a “hard and fast” response that quickly implemented quarantines and immigration restrictions, similar to other countries like Vietnam¹⁶. The New Zealand response implemented an alert system for COVID-19¹⁷ which comprises four levels of increasingly strict interventions. In this case, the four levels can be modelled as a discrete controller⁹ which can interact with the continuous SEIR model as a type of CPS. Such an approach can be used in order to continuously evaluate the efficacy of the control strategy while the pandemic is still in a relatively nascent period and more information is being learned about its dynamics each day.

The use of formal modelling for biological processes has been advocated by Fisher and Henzinger¹⁸, which makes a distinction between computational models and *executable models*. More recently, Bioengineers have adopted an executable model called Hybrid Input-Output Automata (HIOAs)^{10,19} for developing abstract models. These abstractions are used to achieve behaviour from cellular²⁰ to organ levels^{21,22}. These abstract models are also “executable” in the sense that hardware and software implementations may be derived from them so that they work as virtual organs^{21,23,24}.

An HIOA captures both the continuous (i.e. the population model) and discrete (i.e. the government controller) dynamics through the use of an automata with included ODEs. The conversion of the SEIR model into HIOA results in the formal model of Fig. 1b, where the two locations capture whether the Intensive Care Unit

(ICU) capacity has been exceeded. The formal nature of these models means that they can be used in simulation and code generation frameworks with relative ease^{25,26}. We have used the recently developed Intensive Care Unit (ICU)²³, which allows for the specification of a complex network of HIOAs.

To illustrate our methodology we have selected New Zealand and Italy, who have adopted disease management approaches that differ in terms of their response speed—where New Zealand is quick to increase restrictions, Italy takes comparatively longer. We show that in the case of the four-level New Zealand control, we are able to make decisions around the optimal criteria for switching between the control modes to minimise the impact of the virus. Our methodology is generic enough and has the potential to be adopted to other alternative settings.

Results

A simple controller in the New Zealand context. The proposed CCPE approach is first demonstrated using the New Zealand COVID-19 context using a simple controller we term NZ-C1. The NZ-C1 control strategy is to initiate a strong lockdown measure, which is introduced early and is not lifted until the new infections approach zero. We compare against the official data which contains the number of cases (both confirmed and probable), recovered, and deaths for every day from 20th March 2020 to 9th September 2020. Also, on 26th March 2020 (6 days after the first date in our data), the New Zealand government initiated their full lockdown measures, which remained in place until 28th April 2020 when some restrictions began to be eased.

First, we examine the accuracy of our CCPE approach by comparing it to the New Zealand data as a means to increase confidence in our predicted future disease dynamics, as per Fig. 1. In our framework, we propose the modelling of both the plant and controller as HIOA⁹. We create a simple controller (Fig. 1c), which transitions into a lockdown mode (LD) 6 days after the start. The controller modes are depicted as two different states of the system, namely Pre-LD and LD respectively. Within every mode, we encapsulate a condition that determines the maximum time control can reside in a given mode, which is known as the *invariant*. In the LD mode, however, no such invariant is specified. In this case, the invariant is by default `true` and hence control can remain in this location forever. In contrast, control can remain in the Pre-LD mode, when the current time t is less than 6 days. The rate of change of time is modelled as $\text{ODE } \dot{t} = 1$ within both modes.

Transitions between modes happen when some conditions are satisfied. For example, the transition from Pre-LD to LD happens when the current value of t becomes 6. When a transition triggers, some variables are updated. For example, when this transition triggers, the value of time t is reset (by the reset action, which is denoted $t' = 0$). Also the value of R_0 is set to 0.316.

For this model, we use the previously described values for R_0 of 2.5 and 0.316 for pre-lockdown and lockdown respectively. Figure 1d–f show the results of this simulation for three main metrics. By day 120 (19th July 2020) the cases have levelled out in both the real data and model data. On this date, the simulated model predicts 1505 confirmed cases, while in reality there were 1506, an error of only 1 case. Overall, the correlation coefficient is 0.9752.

With this simple controller which remains in lockdown indefinitely (i.e. until a vaccine arrives), the cumulative infection count converges to a realistic number, indicating that the 4 weeks of lockdown was effective at eradicating the disease. This can be seen in Fig. 1e, where the active infections decrease to around zero by day 100, meaning that the disease has been eradicated. Finally, the total number of deaths in this scenario is expected to be 22, which matches up exactly with the official data.

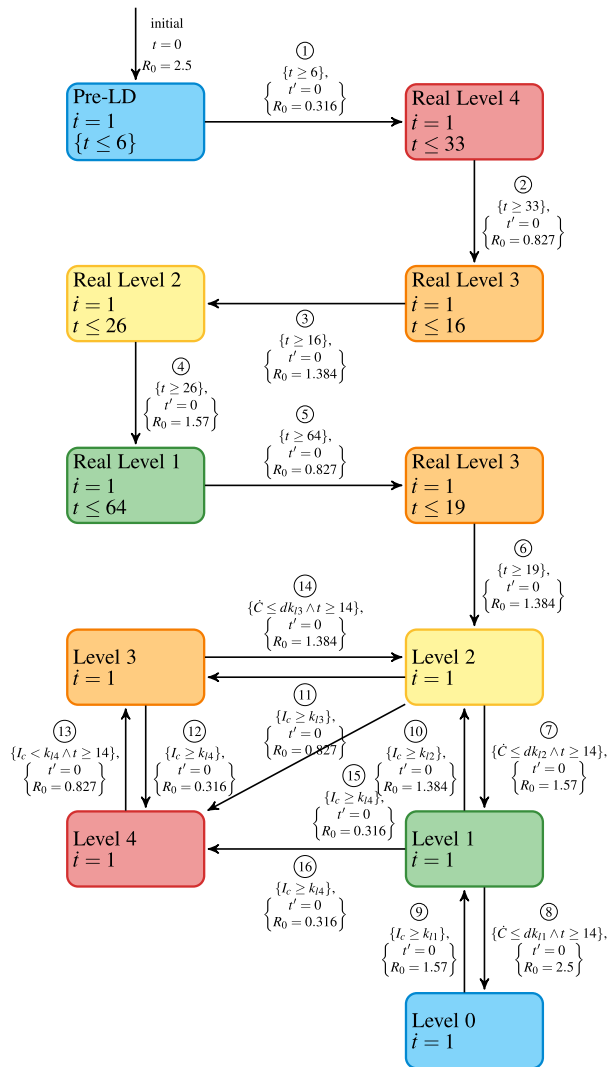
CCPE model of the New Zealand Government control strategy. Next, we investigate the disease dynamics in New Zealand over a longer period of time (600 days) with a more complex model which closely follows the government's strategy of four different levels of increasing stringency, along with their historical changes. The previous controller (Fig. 1c) is extended by incorporating a control policy that reflects these alert levels, where Pre-LD and LD correspond to Level 0 and Level 4 respectively. This new controller is called NZ-C2 and is shown in Fig. 2a. Additionally, the plant model is augmented to allow for the introduction of a “second wave” of infections around day 100 to capture what was experienced in the New Zealand context.

Until 9th September 2020 (day 172) NZ-C2 follows the historical actions of the real-world control strategy. Subsequently, NZ-C2 tries to set the alert level in order to determine an appropriate reproduction number R_0 for the current situation. We have based our work on the reports released by the New Zealand government and the analysis of R_0 values and associated alert levels⁷.

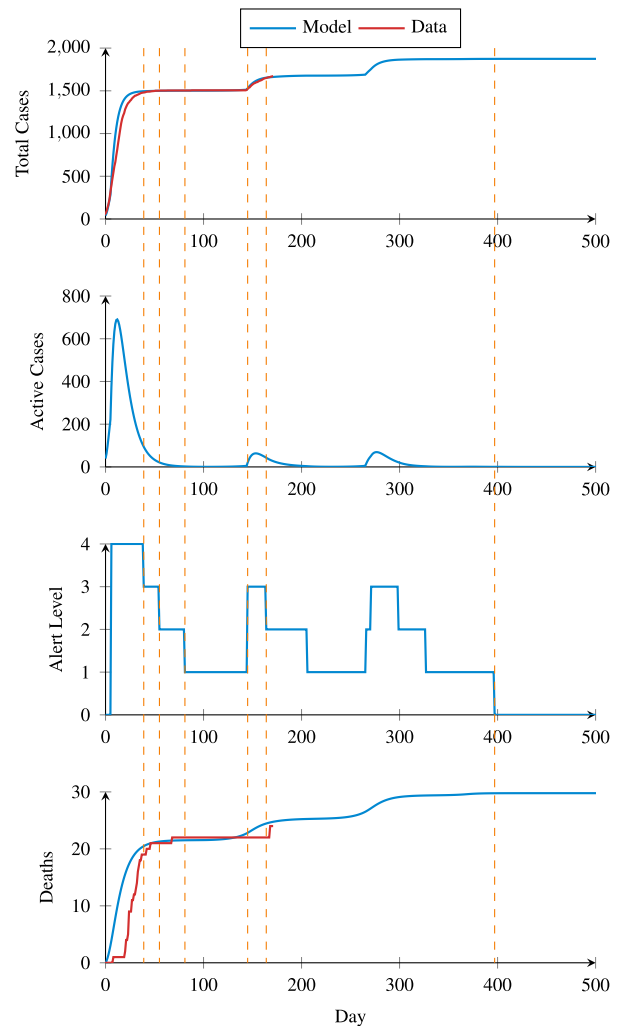
For New Zealand, Table 2 presented in the “Methods” section lists major interventions and their associated relative reproduction number changes indicating how they increase/decrease the R_0 . According to²⁷, the initial value of R_0 is 2.5 without any control, which corresponds to alert level 0 in our model. In summary, the R_0 values for alert levels 4 through 1 are 0.316, 0.827, 1.384, 1.570, respectively. The maximum value of R_0 is 2.5, which corresponds to level 0.

The controller HIOA which captures the transitions between these levels is shown in Fig. 2a. Here, the conditions for increasing the alert level are based on the current number of infected cases (I_c). For example, from level two if $I_c \geq k_{l3}$ then the alert level immediately rises to three. On the other hand, the alert level can go down if the increasing rate of new cases per day (\dot{C}) is less than a certain amount. For example, from level three if $\dot{C} \leq dk_{l3}$ then the alert level decreases to level two. In addition, to avoid frequent oscillations between levels, a minimum duration within a level before being able to drop down to a lower level is added and is set to be 14 days.

The simulation results for this controller are shown in Fig. 2b, where we also include the presence of a vaccine from day 365, which results in the country moving out of all remaining lockdown measures on day 397 (22nd April 2021). In contrast to the scenario of continuing the lockdown based on the previous controller NZ-C1, we observe gradual step downs in the control level. Although there will be 30 deaths, 8 more than the previous



(a) The four-level alert system captured as an HIOA (NZ-C2)



(b) Simulation of COVID-19 spread with vaccine arrival on day 365

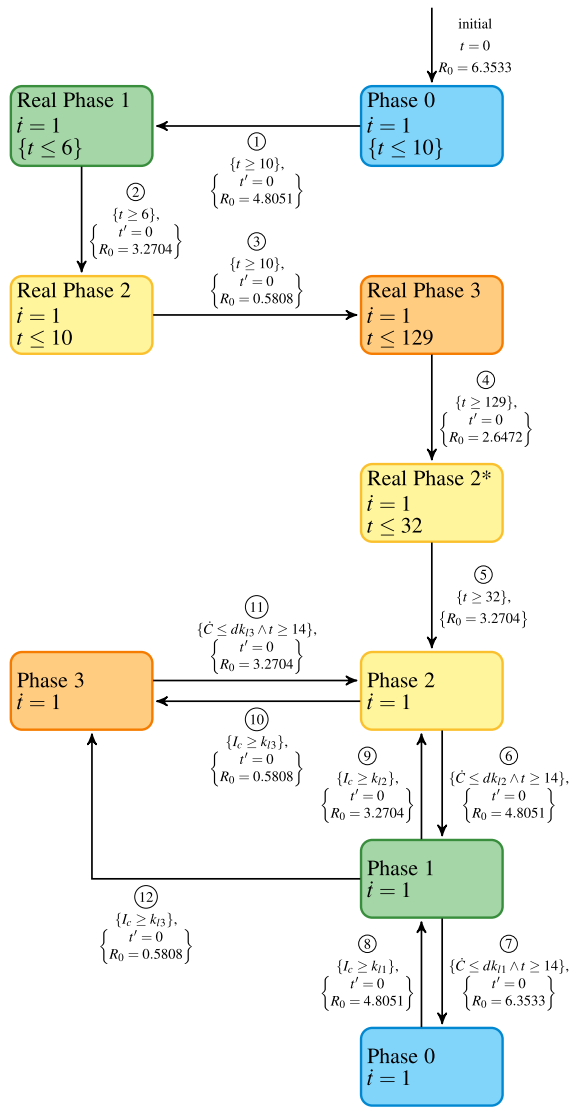
Figure 2. The controller and simulation results corresponding to the New Zealand system for fighting COVID-19.

lockdown scenario, the four-level approach allows for society to begin its return to normalcy from day 39 in order to minimise economic damage relative to the controller NZ-C1 caused as a result of enforced social distancing⁴.

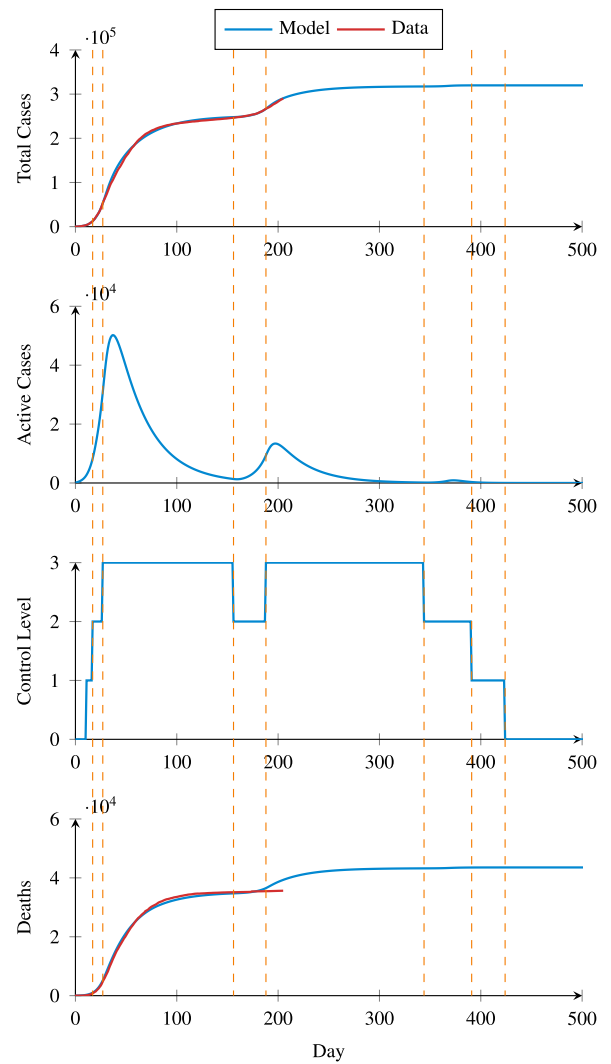
Additionally, the model and controller show their ability to capture both the real-world second wave (at around day 150—18th August 2020)) in a realistic manner, as well potential future outbreaks (from around day 250—18th August 2020)). In these cases, the controller reacts proportionately to the risk associated with the current situation based on both the number of active cases (I_c) and the rate of new cases (\dot{C}).

Modelling Italy’s control strategy. The CCPE approach can be adapted to the intervention techniques of other countries. For example in Italy, the government does not have an explicitly outlined intervention system, instead the control actions are progressively released as they are needed. We use the published *stringency index*¹⁵ for Italy across time in order to create an approximation of their control strategy in our framework. For example, on 23rd February 2020, the stringency index was listed as 66.67, while subsequent measures increased this to 71.43, 90.48, and finally 95.24¹⁵. We create an approximate discrete controller for this approach (Fig. 3a), where the phases correspond to a degrees of stringency mentioned earlier. Note that the date of first observation point in the Italy data is 23rd February 2020.

The control flow of the Italy model called I-C1 in Fig. 3a is as follow. From the initial state Phase 0, transition ① leads to Phase 1. This transition is triggered based on time, according to the historical actions of Italy government. For instance, Italy was in Phase 0 on 23rd February 2020, and moved to Phase 1 by closing the schools and universities on 4th March 2020. Similarly, transitions ②, ③, ④, and ⑤ are triggered based on the time when historical actions were imposed. A countrywide lockdown was issued on 10th March 2020 (day 16) and the nation entered Phase 2. On 20th March 2020 (day 26), the government further tightened the control by reducing the public transportation and initiated Phase 3, before beginning to relax restrictions on 27th



(a) A three-level control system captured as an HIOA (I-C1)



(b) Simulation of COVID-19 with the vaccine arrival on day 365

Figure 3. The controller and simulation results corresponding to the Italy system for fighting COVID-19.

July 2020 (day 155) which allowed for a second wave of infections. For Italy, according to our estimation based on¹⁵, the reproduction number R_0 is 6.3533 in Phase 0, 4.8051 in Phase 1, 3.2704 in Phase 2 (2.6472 in Phase 2*), and 0.5808 in Phase 3.

After the historical transitions have been performed (①–⑤) in Fig. 3a, we apply the same control strategy presented in Fig. 2a. That is, the control level can decrease based on \hat{C} and time remained in a level, or the control level can increase based on I_c . Precisely, the same level changing conditions are used for Italy. In this way, we can examine the performance of the same controller in different countries. We set 10, 5, and 0.01 for dk_{l3} , dk_{l2} , and dk_{l1} , respectively. Also, k_{l3} , k_{l2} , and k_{l1} are 6046, 3023, and 605, respectively. Additionally, the constraint to level four (k_u) is equal to the hospital capacity of approximately 483,694¹⁴.

The simulation results for the Italy model are shown in Fig. 3b. When control goes down to phase two for the first time, the active infection count (I_c) starts to increase again, causing a second wave of infections and necessitating the return to phase three. We can observe that in order to deal with this second wave, the controller implements phase three and remains there until day 344. Overall, the simulation predicts that approximately 45,000 deaths and 320,000 confirmed cases are expected in Italy.

Modelling other controllers. We can examine various “what if” scenarios of COVID-19 in New Zealand, as a result of varying intervention techniques. A simple control policy in previous work has consisted of only two levels, essentially a full lockdown and no control¹⁴. Precisely, a complete lockdown (level four) is triggered if the currently active infection count exceeds the hospital ICU capacity ($\{I_c \geq k_u\}$), while in times where the currently active infection count is less than the half of the hospital capacity ($\{I_c \leq k_u/2\}$), the lockdown is removed (level zero), as shown in Fig. 4a.

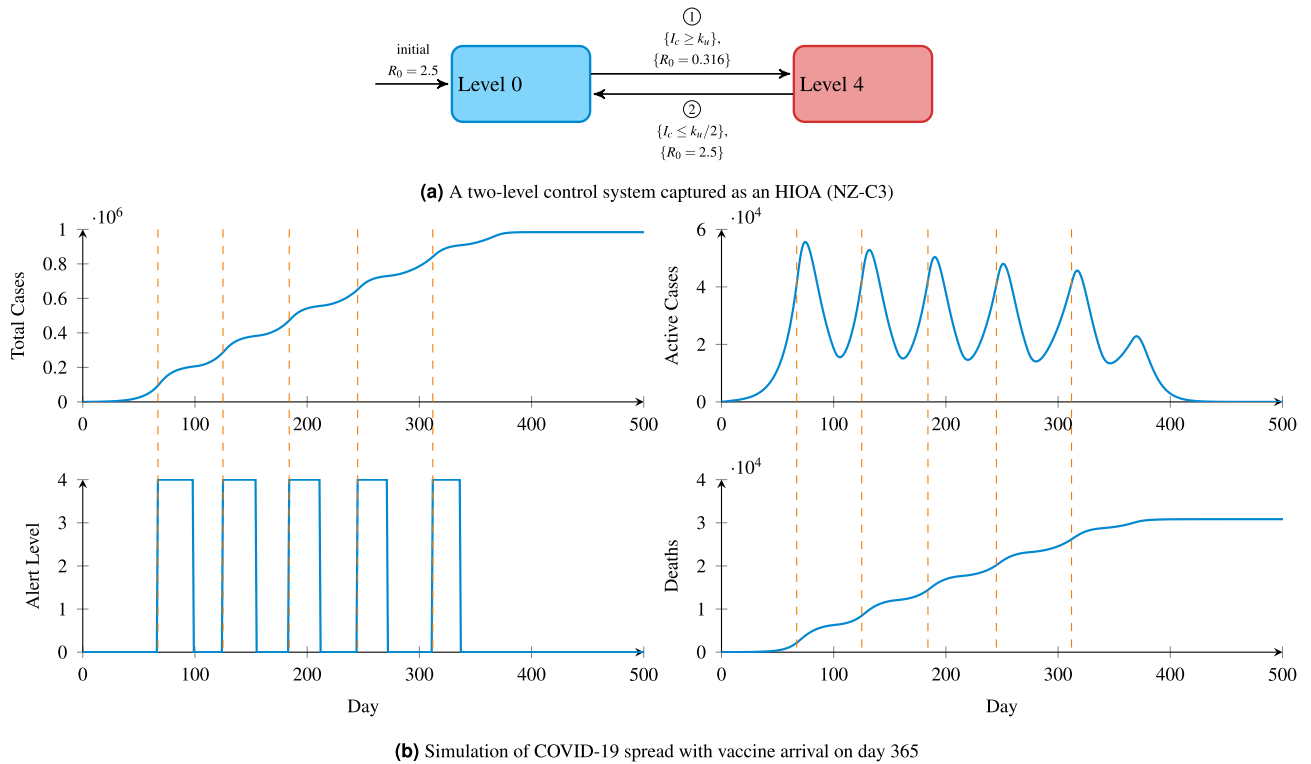


Figure 4. Examples of government interventions with only lockdown action.

Figure	Plant	Controller	Confirmed cases	Deaths	Description	Social impact
1	PL-2	NZ-C1	1501	22	Indefinite lockdown	Lockdown lasts until vaccine is available
2	PL-3	NZ-C2	1874	30	Four level control	Business can operate after day 39, and a near zero infection count is achieved on day 397
4	PL-1	NZ-C3	983,960	30,835	Two level control	Infection count oscillates until it reaches zero on day 481
3	PL-1	I-C1	319,834	43,540	Three level control	A near zero infection count is achieved after 424 days

Table 1. A summary of Compositional Cyber-Physical Epidemiology case studies.

The simulation results for this model in our framework are shown in Fig. 4b. As expected, the control level frequently switches between four and zero as the number of active cases oscillates. This results in a number of 1-month lockdown happening after day 67. Although the peaks of oscillation in the infection case graph gradually diminishes over time, the final number of deaths is extremely high and control remains in the lockdown for a long period of time, causing drastic impacts on the economy.

Discussion

The compositional approach of CCPE allows the flexibility of formal modelling and validation of government control strategies to manage a pandemic. We have shown the ability of CCPE to model the dynamics of COVID-19 in conjunction with the various intervention techniques that governments employ. Table 1 compares the controllers used in this paper. As we can see, in the case of New Zealand, the controller NZ-C2 achieves much better overall outcome compared to the simple controller NZ-C1. While the lockdown for NZ-C1 lasts until a vaccine is available, the economic impact of such a long lockdown may be catastrophic. In contrast, the controller NZ-C2 has a gradual lifting of restrictions, which reaches level 1 much faster. Also, the overall risk of this strategy is a marginal increase in the number of deaths. In contrast to these two controllers, is the third control strategy NZ-C3, which introduces oscillations. We can see immediately the impact of a poorly managed control strategy, which may lead to three orders of magnitude more deaths. Finally, we also present the controller for Italy, which is modelled based on the actions of their government and as reported in¹⁵.

CCPE allows the formal modelling of complex controllers. This enables the systematic evaluation of various control strategies in order to determine the best approach for a country which minimises the economic and social impacts, in addition to achieving the best healthcare outcome. As long as each NPI can be quantified, in terms of R_0 or testing rate, then the importance of individual NPIs can also be evaluated in terms of their overall impact

on pandemic control. These NPIs can then be organised into an overall policy which includes both the NPIs to enforce, the conditions under which they are enforced, and how long they should remain in place.

While the CCPE framework as presented here is based on the SEIR model¹⁴, there is nothing that restricts our framework to such a model. Any continuous model which can be captured through a series of ODEs is able to be used which can open the door to more accurate simulation techniques, such as the enhanced version used by CovidSIM⁵, the recent SIDARTHE model²⁸, or even microscale modelling. We have already shown this ability by suggesting some modification to SEIR to better account for contact tracing and isolation. This is presented in “Methods” section and is denoted as the revised plant model PL-2 in Table 1. Additionally, PL-3 allows for the capturing of the second wave dynamics.

The effectiveness of the CCPE framework relies on the fidelity of the transmission model and parameter estimation, requiring expertise in both epidemiology and statistical analysis, both of which are rapidly changing as our understanding of the pandemic increases. As such, the estimation of R_0 is technically challenging²⁹ and the value varies due to different model assumptions and estimation procedures^{27,30–33}. While the World Health Organization (WHO) estimates that the basic R_0 ranges between 1.4 and 2.5³⁴, Liu et al. suggested that the value is expected to be higher based on evolving research³⁵. To further complicate this matter, cultural differences between countries can have an impact on the effectiveness of NPIs at reducing R_0 , such as social distancing⁴.

To apply the CCPE framework to other countries, the R_0 value should be examined. However, this reproduction number varies based on the control measures implemented by each country^{29,30,36–38}. To investigate the interaction between government interventions and disease transmission dynamics, action-specific R_0 values are essential. Apart from the control actions, many factors, such as population density³⁹, mobility³⁰, and spatial heterogeneity⁴⁰, affect the R_0 value.

The ability for our CCPE framework to work across a range of these different country-specific plant models and various control designs creates a useful tool for designing strategies to fight COVID-19. The analysis of counter-measures and their impact on dealing with the disease has traditionally been limited to simple “if-else” style controllers, and here we show the ability to model counter-measures which are able to include some form of state in their logic.

Outlook

In this work, we evaluated the composition of a controller with an epidemiological model. However, the CCPE framework is far more flexible. HIOA-based modelling can be composed with any number of other HIOA. Further HIOAs could be used which take into account aspects such as legislation, culture, economy structure, administration, etc.^{4,41–43}. For example, an economic model could be added³, which takes into account the various measures being applied in order to provide a metric of the financial toll. Such a model could then be used to design a controller which not just minimises the number of deaths in the population, but also reduces the economic impact in a form of bi-criteria optimisation^{44,45}.

In our work, the criteria used for switching between modes of the controller were based on comparing the number of active cases to the ICU capacity. Instead, control mechanisms could be created which take into account additional information, such as the climate, to more accurately capture the decision-making process. Moreover, we could further refine the dynamical modes to better represent the rate of testing.

Finally, a robust estimation approach of action specific R_0 values within context of geographical and social heterogeneity should be systematically investigated in the future. COVID-19 is still relatively new and there exists a large variation in potential reproduction numbers between studies. We note that the accuracy of any epidemiological model depends on the accuracy of its reproduction number, and so further improvements in this area would be of great benefit. For example, there is the potential for the adoption of an approach as recently proposed in¹³ if the reproduction number could be approximated as a continuous function. While this is a challenging proposition, our work opens the door for more engineering researchers to create an impact on current and future pandemics. A momentum is already in evidence as reported in⁴⁶ to show how Engineers are coming together to contribute to this cause in various ways.

Methods

The SEIR model of COVID-19. The modified SEIR model¹⁴ consists of variables which represent the various sub-populations during an epidemic: susceptible (S), exposed (E), pre-symptomatic (P), infectious (I), recovered (R), and deaths (D). The infectious and recovered cases are further categorized into untested (I_u, R_u) and confirmed (I_c, R_c). The dynamics of the transmission between these sub-populations can be described by a series of coupled ODEs, shown in Eq. (1) through (8).

$$\frac{dS}{dt} = -\beta S(\epsilon P + I_u + I_c) \quad (1)$$

$$\frac{dE}{dt} = \beta S(\epsilon P + I_u + I_c) - \alpha E \quad (2)$$

$$\frac{dP}{dt} = \alpha E - \delta P \quad (3)$$

$$\frac{dI_u}{dt} = \delta P - (\gamma + c)I_u \quad (4)$$

$$\frac{dI_c}{dt} = cI_u - \gamma I_c \quad (5)$$

$$\frac{dR_u}{dt} = \gamma(1 - CFR)I_u \quad (6)$$

$$\frac{dR_c}{dt} = \gamma(1 - CFR)I_c \quad (7)$$

$$D = 1 - S - E - P - I_u - I_c - R_u - R_c \quad (8)$$

The Case Fatality Ratio (CFR) depends on the number of active people in the ICU and the ICU capacity. If the number of active people in the ICU is within the ICU capacity then the CFR is simply equal to some lower bound CFR_0 (1%). When this limit is exceeded, the CFR is decided by a mixture of patients who are receiving ICU care (CFR_0) and those who are not (CFR_1). The result of this is a piecewise function as in Eq. (10) where CFR_1 (2%) is the maximum fatality rate, n_{ICU} denotes the maximum ICU beds, N is the population size, and p_{ICU} is the proportion of total cases which require ICU attention.

$$patients = N \times (I_u + I_c) \times p_{ICU} \quad (9)$$

$$CFR = \begin{cases} CFR_0 & \text{if } patients \leq n_{ICU} \\ CFR_1 - (CFR_1 - CFR_0) \times \frac{n_{ICU}}{patients} & \text{otherwise} \end{cases} \quad (10)$$

The SEIR model can be described as HIOA, shown earlier in Fig. 1b. X is the vector of all epidemic variables initialized to X_0 , A is the matrix of the parameters, and $\dot{X} = AX$ is the matrix representation of Eqs. (1) through (8). When the ICU demand N_{icu} is less than or equal to the maximum ICU capacity n_{ICU} , the HIOA stays in the location *Below ICU* with CFR of CFR_1 . Otherwise, control goes to the location *Beyond ICU* and the CFR is defined by Eq. (10).

In the model (Eq. 1, 2), the reproduction number R_0 determines the transmission rate β as per Eq. (11). Here, ϵ is the relative infectiousness in the presymptomatic period, δ is the transition rate from presymptomatic to infectious, and γ is the transition rate from infectious to recovered.

$$\beta = \frac{R_0}{\epsilon/\delta + 1/\gamma} \quad (11)$$

These transition rates are decided by the virus nature, while R_0 depends on the contacts and the transmissibility¹². The government control measures can impact this reproduction number, and hence also β , by reducing:

- physical contacts (e.g. travel restriction, self-isolation, work at home, close schools, etc.), or
- the transmissibility (e.g. hand washing, public disinfection efforts, etc.)

In order to start the propagation of the disease through the population we start with an initial number of cases (I_c) which matches with the initial number of reported cases. Typically, our simulations start after a country has reached 100 total cases as this is a likely point where local transmission, if not community transmission, has started to occur. Additionally, this allows us to isolate the population from the rest of the world and ignore the potential inflow and outflow of infected people as travel is heavily restricted by this point in time.

We propose a revision of the recent SEIR model¹⁴ in this paper to account for better management of the pandemic using improved case isolation and contact tracing. In Table 1, we denote the SEIR model¹⁴ as the plant model PL-1 while our revised model is marked as the plant model PL-2. This is since case isolation and contact tracing could significantly reduce R_0 for identified cases (i.e. I_c)³⁷. We use different parameters for the transmission rate β (Eqs. 1, 2) such that the confirmed cases have lower transmissivity due to the combined effects of isolation and contact tracing. The resultant refined model replaces Eq. (1) and (2) with Eq. (12) and (13).

$$\frac{dS}{dt} = -\beta_1 S(\epsilon P + I_u) - \beta_2 S I_c \quad (12)$$

$$\frac{dE}{dt} = \beta_1 S(\epsilon P + I_u) + \beta_2 I_c - \alpha E \quad (13)$$

Further, to capture the the dynamics of externally introduced second waves we create a further extended plant model named PL-3. This model, at some predefined time t_2 will instantly move a set number of people from the susceptible population (S) into the exposed population (E). Such a model is required in the context of New

Intervention	Weight	Level 4	Level 3	Level 2	Level 1	Level 0
Widespread testing	0.186	✓	✓	✓	✓	✗
Temperature checkpoints	0.093	✓	✓	✓	✓	✗
Contact tracing	0.186	✓	✓	✓	✓	✗
Close contacts of confirmed cases ordered to self-isolate	0.093	✓	✓	✓	✓	✗
Large scale disinfection efforts	0.046	✓	✓	✓	✗	✗
Distribution of PPE to at-risk workers	0.093	✓	✓	✓	✓	✗
Hygiene public awareness efforts	0.186	✓	✓	✓	✓	✗
International travel ban	0.186	✓	✓	△	✗	✗
Domestic travel restrictions	0.093	✓	✓	△	✗	✗
People forced to remain home	0.186	✓	✗	✗	✗	✗
Bans on outdoor gatherings over 500 people	0.093	✓	✓	✓	✓	✗
Bans on indoor gatherings over 100 people	0.093	✓	✓	✗	✗	✗
Bans on recreational sports	0.046	✓	✓	✗	✗	✗
Bars and restaurants close	0.186	✓	△	✗	✗	✗
Schools close	0.186	✓	△	✗	✗	✗
Tertiary education facilities close	0.093	✓	△	✗	✗	✗
Small food retailers close	0.093	✓	✗	✗	✗	✗
Non-essential retail business close	0.093	✓	△	✗	✗	✗
Summation		2.184	1.673	1.116	0.930	0
Base reproduction number (R_0)		2.5	2.5	2.5	2.5	2.5
Final R value		0.316	0.827	1.384	1.570	2.5

Table 2. A list of the interventions involved at each alert level in New Zealand, and the reproduction number derivation. A tick (✓) represents that an intervention is applied, a cross (✗) means that it is not applied, and a triangle (△) is used when an intervention is partially applied.

Zealand, where it is most likely that eradication of the virus was achieved prior to the emergence of the second wave and thus the cause of this re-emergence was most likely external.

The New Zealand model of COVID-19. For the epidemiological model of New Zealand, we use base reproduction number of 2.5 as is widely reported without control measures in place²⁷. To investigate the interaction between government interventions and disease transmission dynamics, we need to introduce various reproduction numbers for the different action control strategies and stages. The estimation of R_0 is technically challenging²⁹ and a number of studies have been done^{31,32,35,38,47}. However, these values are not specific to certain control policies.

We identified which interventions are applied in the New Zealand alert levels, indicated in Table 2 by a tick (✓) or a cross (✗) to capture if a given intervention is applied (respectively not applied) in a given alert level. Each intervention is also weighted in its effectiveness, with the weighted sum being 2.184. A triangle (△) is used when an intervention is partially applied. In this case, half the weight is considered. At the bottom of Table 2, we show the calculated reproduction numbers for each alert level by taking into account both the base reproduction number R_0 and the interventions applied. In summary, the R_0 values for alert levels 4 through 1 are 0.316, 0.827, 1.384, 1.570 respectively. The maximum value of R_0 is 2.5, which corresponds to level 0. Additionally, for use with the previously described PL-2 model, we impose an R_0 value of 0.02 for confirmed cases to capture the enforced isolation placed upon them.

In order to capture the increased testing rates (and more rigorous contact tracing) associated with higher alert levels, we also vary the value c used to represent the testing rate in PL-3. In this model, we use daily rates of 0.3, 0.2, 0.15 and 0.01 for alert levels 4 through 1, respectively.

The controller NZ-C2, in Fig. 2a, matches a given alert level to its corresponding R_0 value. Initially, the control starts from Pre-LD and move to LD just like the previous controller in Fig. 1c. After 33 days this corresponds

Phase	Phase 0	Phase 1	Phase 2	Phase 3	Phase 2*
Date range	23 Feb–4 Mar	4 Mar–10 Mar	10 Mar–20 Mar	20 Mar–27 Jul	27 Jul–28 Aug
R_0	6.3533	4.8051	3.2704	0.5808	2.6472

Table 3. Estimated reproduction numbers for each phase in Italy.

to 27th April 2020, which is the scheduled start of Level 3. After this point, the control enters Level 3, and the reproduction number is set to 0.827. The transitions ① through ⑥ are taken based on time, like NZ-C1, since these mimic known time based government actions.

Subsequently, the government decisions, which are yet unknown, will have to be mimicked using more complex mechanisms. We use the following strategy to determine the transition conditions, which will not be time based alone, as follows. First we denote the rate of new cases per day as \dot{C} and the current number of infected cases is I_c . We consider the following parameter values based on the published data from New Zealand¹⁴. We set k_{I_4} , k_{I_3} , k_{I_2} , and k_{I_1} as 100, 50, 5, and 1, respectively. dk_{I_3} , dk_{I_2} , and dk_{I_1} are 10, 5, and 0.01, respectively. Finally, in our results, we assume that a vaccine will arrive 365 days after 20th March 2020. At this time, the number of susceptible people progressively decreases to zero, assuming widespread adoption of an effective vaccine.

The conditions for increasing the alert level are based on the current number of infected cases (I_c). For example, from level two if $I_c \geq k_{I_3}$ then the alert level immediately rises to three. On the other hand, the alert level can go down if the increasing rate of new cases per day (\dot{C}) is less than a certain amount. For example, from level three if $\dot{C} \leq dk_{I_3}$ then the alert level decreases to level two. In addition, to avoid frequent oscillations between levels, a minimum duration within a level before being able to drop down to a lower level is added, and is set to be 14 days.

The Italy model of COVID-19. Unlike New Zealand, Italy does not issue a systemic intervention strategy for COVID-19. Instead, the government releases the actions incrementally as they are needed. The Oxford COVID-19¹⁵ provides a stringency index of the measures taken by various governments around the world. According to the stringency index of Italy's interventions, we divide the transmission trajectory into four phases. Considering that the initially reported cases are mostly imported rather than community transmission, the starting point of the analysis is 23rd February 2020, when the reported number of cases is 155. As a first attempt, we use the SEIR model¹⁴ and curve fitting to estimate policy-specific reproduction numbers for Italy. We use the MATLAB function `lsqcurvefit` to search for these reproduction numbers for each phase by minimizing the square of the residual error between the SEIR simulation and the reported data⁴⁸. The resulting reproduction numbers are listed in Table 3.

The controller is shown in Fig. 3a. For dropping alert levels, we have values of 10, 5, and 0.01 for dk_{I_3} , dk_{I_2} , and dk_{I_1} respectively. The population of Italy (N) is 60,461,828 and we have level changing constraints of 6046,3023, and 605 for k_{I_3} , k_{I_2} , and k_{I_1} , respectively.

HAML. Hybrid Automata Modelling Language (HAML)²³ is a recently developed tool in our group for the compositional modelling and verification of CPSs. To create the CCPE system in HAML we simply create two automata, one each for the plant and controller, and compose them as a single network. For the plant model, Listing 1a, we have an automata with an input R_0 value which is used to determine the rate of reproduction in the model. Additionally, there are two outputs for the number of currently infected (and tested) people, I_c , and the rate of change in the number of cases (C_{dot}). The two locations of Fig. 1b are shown which have the same flow constraints but differ in their calculation of the CFR to create a piecewise implementation of Eq. (10) through the use of update constraints.

The discrete controller has external inputs and outputs which mirror those of the plant model, having two inputs, I_c and C_{dot} , and a single output, R_0 . Listing 1b shows this controller captured in HAML, using locations for each of discrete modes that it can be in. When the number of current confirmed cases (I_c) reaches an upper bound for each location then the control progresses to a higher alert level, while when the change in number of cases (C_{dot}) reaches a lower bound then control transitions to a lower alert level. The values of R_0 for each control location are taken from Table 2.

Finally, composition between these two components simply requires mapping their respective inputs and outputs together. This is achieved by defining each of the previous models, creating a single instance for each, and then providing the mapping of their variables, as shown in Listing 1c.

```

1  inputs:
2    R0: REAL
3
4  outputs:
5    Ic: REAL
6    C_dot: REAL
7
8  parameters:
9    N: REAL
10   eps: REAL
11   alpha: REAL
12   delta: REAL
13   gamma: REAL
14   CFR0: REAL
15   CFR1: REAL
16   n_ICU: REAL
17   p_ICU: REAL
18
19  locations:
20  below_ICU:
21    invariant: patients <= n_ICU
22    flow:
23      S: -beta * S * (eps * P + Iu + Ic)
24      E: beta * S * (eps * P + Iu + Ic) - alpha * E
25      P: alpha * E - delta * P
26      Iu: delta * P - (gamma + c) * Iu
27      Ic: c * Iu - gamma * Ic
28      Ru: gamma * (1 - CFR) * Iu
29      Rc: gamma * (1 - CFR) * Ic
30      D: gamma * CFR * (Iu + Ic)
31      C: c * Iu
32    update:
33      beta: R0 / (eps / delta + 1 / gamma)
34      C_dot: c * Iu
35      patients: N * (Iu + Ic) * p_ICU
36      CFR: CFR0
37    transitions:
38      - to: beyond_ICU
39      guard: patients > n_ICU
40  beyond_ICU:
41    invariant: patients > n_ICU
42    flow:
43      S: -beta * S * (eps * P + Iu + Ic)
44      E: beta * S * (eps * P + Iu + Ic) - alpha * E
45      P: alpha * E - delta * P
46      Iu: delta * P - (gamma + c) * Iu
47      Ic: c * Iu - gamma * Ic
48      Ru: gamma * (1 - CFR) * Iu
49      Rc: gamma * (1 - CFR) * Ic
50      D: gamma * CFR * (Iu + Ic)
51      C: c * Iu
52    update:
53      beta: R0 / (eps / delta + 1 / gamma)
54      C_dot: c * Iu
55      patients: N * (Iu + Ic) * p_ICU
56      CFR_d: CFR1 - CFR0
57      CFR: CFR1 - CFR_d * n_ICU / patients
58    transitions:
59      - to: below_ICU
60      guard: patients <= n_ICU

```

(a) SEIR model specification for PL-1 (Figure 1b)

```

1  inputs:
2    Ic: REAL
3    C_dot: REAL
4
5  outputs:
6    R0: REAL
7    Level: REAL
8
9  parameters:
10   k_L4:
11     type: REAL
12     default: 40000
13   R0_L0:
14     type: REAL
15     default: 2.5
16   R0_L4:
17     type: REAL
18     default: 0.316
19
20  locations:
21  Level0:
22    invariant: Ic < k_L4
23    update:
24      R0: R0_L0
25      Level: 0
26    transitions:
27      - to: Level4
28      guard: Ic >= k_L4
29  Level4:
30    invariant: Ic > k_L4 / 2
31    update:
32      R0: R0_L4
33      Level: 4
34    transitions:
35      - to: Level0
36      guard: Ic <= k_L4 / 2
37
38  initialisation:
39    state: Level0

```

(b) Controller specification (NZ-C3) (Figure 4a)

```

1  name: nz-c3
2
3  system:
4    definitions:
5      Plant: !include ../plants/pl1.yaml
6              (Listing 1a)
7      Controller: !include ../controllers/nz-c3.yaml
8                  (Listing 1b)
9    instances:
10     Plant:
11       type: Plant
12       parameters:
13         vaccine_arrival_date: 365
14     Controller: Controller
15
16  mappings:
17     Plant.R0: Controller.R0
18     Controller.Ic: Plant.Ic
19     Controller.C_dot: Plant.C_dot

```

(c) Network specification for NZ-C3 (Figure 1a)

Listing 1. Example HAML specifications for the Compositional Cyber-Physical Epidemiology system.

Data availability

Accession codes All models and code used for this work are publicly available on GitHub: <https://github.com/PRETgroup/ccpe-covid19>. The real-world data used to validate our models was obtained from the publicly available dataset of Johns Hopkins CCSE: <https://github.com/CSSEGISandData/COVID-19>.

Received: 30 April 2020; Accepted: 19 October 2020

Published online: 11 November 2020

References

- World Health Organization. Coronavirus disease (COVID-19): Weekly epidemiological update. Technical documents, World Health Organization (2020).
- Humanity tested. *Nat. Biomed. Eng.* **4**, 355–356. <https://doi.org/10.1038/s41551-020-0553-6> (2020).
- Thunstrom, L., Newbold, S., Finnoff, D., Ashworth, M. & Shogren, J. The benefits and costs of flattening the curve for covid-19. *SSRN Electron. J.* <https://doi.org/10.2139/ssrn.3561934> (2020).
- Huynh, T. Does culture matter social distancing under the COVID-19 pandemic?. *Saf. Sci.* **130**, 104872. <https://doi.org/10.1016/j.ssci.2020.104872> (2020).
- Wilson, N. *et al.* Modelling the potential health impact of the covid-19 pandemic on a hypothetical European country. *medRxiv* <https://doi.org/10.1101/2020.03.20.20039776> (2020).
- Panovska-Griffiths, J. Can mathematical modelling solve the current covid-19 crisis?. *BMC Public Health* **20**, 551. <https://doi.org/10.1186/s12889-020-08671-z> (2020).
- Castalia. After the lockdown. <https://castalia-advisors.com/blog-after-the-lockdown/> (2020).
- Lee, E. Cyber physical systems: Design challenges. In *2008 11th IEEE International Symposium on Object and Component-Oriented Real-Time Distributed Computing (ISORC)*, 363–369. <https://doi.org/10.1109/ISORC.2008.25> (2008).
- Alur, R. *Principles of Cyber-Physical Systems* (MIT Press, New York, 2015).
- Jiang, Z., Pajic, M. & Mangharam, R. Cyber-physical modeling of implantable cardiac medical devices. *Proc. IEEE* **100**, 122–137. <https://doi.org/10.1109/JPROC.2011.2161241> (2012).
- Anderson, R. & May, R. Population biology of infectious diseases: Part i. *Nature* **280**, 361–367. <https://doi.org/10.1038/280361a0> (1979).
- Weiss, H. H. The sir model and the foundations of public health. *Mater. Mat.* **2013**, 20 (2013).
- Stewart, G., Heusden, K. & Dumont, G. How control theory can help us control covid-19. *IEEE Spectr.* **57**, 22–29. <https://doi.org/10.1109/MSPEC.2020.9099929> (2020).
- James, A., Hendy, S., Plank, M. & Steyn, N. Suppression and mitigation strategies for control of covid-19 in New Zealand. *medRxiv* <https://doi.org/10.1109/10.1101/2020.03.26.20044677> (2020).
- Hale, T. *et al.* Variation in government responses to covid-19. <https://doi.org/10.2139/ssrn.35619340> (2020).
- Huynh, T. The covid-19 containment in Vietnam—what are we doing?. *J. Glob. Health* **10**, 010338. <https://doi.org/10.2139/ssrn.35619341> (2020).
- Ministry of Health NZ. New Zealand covid-19 alert levels. <https://doi.org/10.2139/ssrn.35619342> (2020).
- Fisher, J. & Henzinger, T. Executable cell biology. *Nat. Biotechnol.* **25**, 1239–1249. <https://doi.org/10.2139/ssrn.35619343> (2007).
- Chen, T., Diciolla, M., Kwiatkowska, M. & Mereacre, A. Quantitative verification of implantable cardiac pacemakers over hybrid heart models. *Inf. Comput.* **236**, 87–101. <https://doi.org/10.2139/ssrn.35619344> (2014).
- Ai, W. *et al.* A parametric computational model of the action potential of pacemaker cells. *IEEE Trans. Biomed. Eng.* **65**, 123–130. <https://doi.org/10.2139/ssrn.35619345> (2017).
- Ai, W., Patel, N., Roop, P., Malik, A. & Trew, M. Closing the loop: Validation of implantable cardiac devices with computational heart models. *IEEE J. Biomed. Health Inform.* **24**, 1579–1588. <https://doi.org/10.2139/ssrn.35619346> (2019).
- Wang, L., Malik, A., Roop, P., Cheng, L. & Paskaranandavadivel, N. A formal approach for scalable simulation of gastric ICC electrophysiology. *IEEE Trans. Biomed. Eng.* **66**, 3320–3329. <https://doi.org/10.2139/ssrn.35619347> (2019).
- Allen, N. & Roop, P. Semantics-directed hardware generation of hybrid systems. In *2020 ACM/IEEE 11th International Conference on Cyber-Physical Systems (ICCP)*, 259–268. <https://doi.org/10.1109/ICCP48487.2020.00037> (2020).
- Yip, E. *et al.* Towards the emulation of the cardiac conduction system for pacemaker testing. *ACM Trans. Cyber Phys. Syst.* <https://doi.org/10.1145/3134845> (2016).
- Malik, A., Roop, P., Andalamp, S., Trew, M. & Mendler, M. Modular compilation of hybrid systems for emulation and large scale simulation. *ACM Trans. Embedded Comput. Syst.* **16**, 1–21. <https://doi.org/10.1145/3126536> (2017).
- Allen, N. *et al.* Modular code generation for emulating the electrical conduction system of the human heart. In *2016 Design, Automation Test in Europe Conference Exhibition (DATE)*, 648–653. https://doi.org/10.3850/9783981537079_0187 (2016).
- Imai, N. *et al.* Report 3: Transmissibility of 2019-ncov (Imperial College London, London, 2020).
- Giordano, G. *et al.* Modelling the covid-19 epidemic and implementation of population-wide interventions in Italy. *Nat. Med.* **26**, 855–860. <https://doi.org/10.1038/s41591-020-0883-7> (2020).
- Viceconte, G. & Petrosillo, N. Covid-19 r0: Magic number or conundrum?. *Infect. Dis. Rep.* <https://doi.org/10.4081/idr.2020.8516> (2020).
- Chinazzi, M. *et al.* The effect of travel restrictions on the spread of the 2019 novel coronavirus (2019-ncov) outbreak. *medRxiv* <https://doi.org/10.1101/2020.02.09.20021261> (2020).
- Kucharski, A. *et al.* Early dynamics of transmission and control of covid-19: A mathematical modelling study. *Lancet. Infect. Dis.* **20**, 553–558. [https://doi.org/10.1016/S1473-3099\(20\)30144-4](https://doi.org/10.1016/S1473-3099(20)30144-4) (2020).
- Yuan, J., Li, M., Lv, G. & Lu, Z. Monitoring transmissibility and mortality of covid-19 in Europe. *Int. J. Infect. Dis.* **95**, 311–315. <https://doi.org/10.1016/j.ijid.2020.03.050> (2020).
- Ki, M. Epidemiologic and characteristics of early cases with novel coronavirus (2019-ncov) disease in Republic of Korea. *Epidemiol. Health.* <https://doi.org/10.4178/epih.e2020007> (2019).
- World Health Organization. Statement on the second meeting of the international health regulations (2005) emergency committee regarding the outbreak of novel coronavirus (2019-ncov). [https://www.who.int/news-room/detail/30-01-2020-statement-on-the-second-meeting-of-the-international-health-regulations-\(2005\)-emergency-committee-regarding-the-outbreak-of-novel-coronavirus-\(2019-ncov\)](https://www.who.int/news-room/detail/30-01-2020-statement-on-the-second-meeting-of-the-international-health-regulations-(2005)-emergency-committee-regarding-the-outbreak-of-novel-coronavirus-(2019-ncov)) (2020).
- Gayle, A., Wilder-Smith, A. & Rocklöv, J. The reproductive number of covid-19 is higher compared to sars coronavirus. *J. Travel Med.* <https://doi.org/10.1093/jtm/taaa021> (2020).
- Park, S., Sun, K., Viboud, C., Grenfell, B. & Dushoff, J. Potential roles of social distancing in mitigating the spread of coronavirus disease 2019 (covid-19) in South Korea. *medRxiv* <https://doi.org/10.1101/2020.03.27.20045815> (2020).
- Ferretti, L. *et al.* Quantifying sars-cov-2 transmission suggests epidemic control with digital contact tracing. *Science* **368**, eabb6936. <https://doi.org/10.1126/science.abb6936> (2020).
- Abbott, S. *et al.* Estimating the time-varying reproduction number of sars-cov-2 using national and subnational case counts [version 1; peer review: Awaiting peer review]. *Wellc. Open Res.* **5**, 112. <https://doi.org/10.12688/wellcomeopenres.16006.1> (2020).

39. Hu, H., Nigmatulina, K. & Welkhoff, P. The scaling of contact rates with population density for the infectious disease models. *Math. Biosci.* **244**, 125–134. <https://doi.org/10.1016/j.mbs.2013.04.013> (2013).
40. Ng, T.-C. & Wen, T.-H. Spatially adjusted time-varying reproductive numbers: Understanding the geographical expansion of urban dengue outbreaks. *Sci. Rep.* **9**, 19172. <https://doi.org/10.1038/s41598-019-55574-0> (2019).
41. Lenert, L. & McSwain, B. Balancing health privacy, health information exchange and research in the context of the covid-19 pandemic. *J. Am. Med. Inform. Assoc.* **27**, 963–966. <https://doi.org/10.1093/jamia/ocaa039> (2020).
42. Habibi, R. *et al.* Do not violate the international health regulations during the covid-19 outbreak. *Lancet* **395**, 664–666. [https://doi.org/10.1016/S0140-6736\(20\)30373-1](https://doi.org/10.1016/S0140-6736(20)30373-1) (2020).
43. Gostin, L., FRIEDMAN, E. & WETTER, S. Responding to covid-19: How to navigate a public health emergency legally and ethically. *Hastings Cent. Rep.* **50**, 8–12. <https://doi.org/10.1002/hast.1090> (2020).
44. The White House. Opening up america again. <https://www.whitehouse.gov/openingamerica/> (2020).
45. Guesnerie, R. Pareto optimality in non-convex economies. *Econometrica* **43**, 1–29. <https://doi.org/10.2307/1913410> (1975).
46. Nordrum, A. & Strickland, E. Engineering during a pandemic. *IEEE Spectr.* **57**, 6–7. <https://doi.org/10.1109/MSPEC.2020.9078401> (2020).
47. Alimohamadi, Y., Taghdir, M. & Sepandi, M. The estimate of the basic reproduction number for novel coronavirus disease (covid-19): A systematic review and meta-analysis. *J. Prev. Med. Public Health* **c53**, 151–157. <https://doi.org/10.3961/jpmph.20.076> (2020).
48. Dong, E., Du, H. & Gardner, L. An interactive web-based dashboard to track covid-19 in real time. *Lancet. Infect. Dis.* **20**, 533–534. [https://doi.org/10.1016/S1473-3099\(20\)30120-1](https://doi.org/10.1016/S1473-3099(20)30120-1) (2020).

Author contributions

P.S.R. conceived of the concept. In particular, he formulated the hypothesis based on the research gap. All authors conceived the experiments, J.W.R., N.A., and W.A. conducted the experiments, and J.W.R. and W.A. analysed the results. All authors reviewed the manuscript, where D.P. provided the epidemiological context.

Competing interests

The authors declare no competing interests.

Additional information

Correspondence and requests for materials should be addressed to P.S.R.

Reprints and permissions information is available at www.nature.com/reprints.

Publisher's note Springer Nature remains neutral with regard to jurisdictional claims in published maps and institutional affiliations.



Open Access This article is licensed under a Creative Commons Attribution 4.0 International License, which permits use, sharing, adaptation, distribution and reproduction in any medium or format, as long as you give appropriate credit to the original author(s) and the source, provide a link to the Creative Commons licence, and indicate if changes were made. The images or other third party material in this article are included in the article's Creative Commons licence, unless indicated otherwise in a credit line to the material. If material is not included in the article's Creative Commons licence and your intended use is not permitted by statutory regulation or exceeds the permitted use, you will need to obtain permission directly from the copyright holder. To view a copy of this licence, visit <http://creativecommons.org/licenses/by/4.0/>.

© The Author(s) 2020